

引用格式: ZHENG Yujun, XU Weiwei, LI Xin, et al. Image Quality Evaluation Method for Optical Remote Sensing Satellite Based on an Array of Point Sources[J]. Acta Photonica Sinica, 2023, 52(4):0428001

郑昱君,徐伟伟,李鑫,等. 基于阵列点源的光学遥感卫星像质评价方法[J]. 光子学报, 2023, 52(4):0428001

基于阵列点源的光学遥感卫星像质评价方法

郑昱君^{1,2}, 徐伟伟¹, 李鑫¹, 司孝龙¹, 杨宝云¹, 张黎明¹

(1 中国科学院合肥物质科学研究院 通用光学定标与表征技术重点实验室, 合肥 230031)

(2 中国科学技术大学, 合肥 230026)

摘 要:提出一种基于阵列点源的光学遥感卫星像质评价方法,以轻小型、自动化的反射点源阵列作为检测参照目标,最小二乘法二维高斯模型拟合阵列点源影像获得像点坐标,结合地面点源位置测量获得遥感器地面像元分辨率;以点源影像像点坐标为基准,对阵列点源遥感影像数据进行位置配准与高斯模型拟合获得成像系统点扩散函数与调制传递函数值。试验结果表明:像点坐标的共线误差小于 0.002 像素,地面像元分辨率的相对偏差优于 6.5%,阵列点源可以综合实现光学遥感卫星的像质评价与辐射定标。

关键词:遥感;像质评价;调制传递函数;地面像元分辨率;阵列点源

中图分类号: TP79;O435

文献标识码: A

doi: 10.3788/gzxb20235204.0428001

0 引言

随着光学遥感技术的发展与新一代综合遥感体系的建设实施,卫星遥感数据在自然资源调查、生态环境保护、城市规划建设和测绘制图等领域有越来越广泛的应用,这对遥感数据质量评价精度提出了更高的要求^[1]。地面像元分辨率与调制传递函数(Modulation Transfer Function, MTF)是光学遥感卫星图像质量评价的重要参数,表征遥感器对目标细节的分辨能力以及不同空间尺度目标,尤其是小尺度目标的调制传递特性,在高空间分辨率光学遥感卫星的目标识别与判读、图像解译与信息提取等方面具有重要意义^[2-5]。

目前,光学遥感卫星图像质量评价多采用三线靶标法、辐射状靶标法、倾斜刃边法、阵列点源法等,光学遥感卫星 Quickbird、Worldview 系列、ZY 系列与高分系列等多采用这些方法进行地面像元分辨率与调制传递函数的在轨检测,均取得了一定的在轨检测成效^[6-10]。利用三线靶标或辐射状靶标进行地面像元分辨率检测时,易受采样相位与轨道倾角以及人工判读或解译辐射状靶标遥感影像的可分辨-不可分辨分界点等因素影响,检测精度不高^[5];三线靶标法进行在轨 MTF 检测时,需要布设多组非整数像素间隔的三线靶标,仅能够获取单点(奈奎斯特频率)MTF 值,易受噪声与大气影响^[4,11],且具有一定的离散性;倾斜刃边法所布设的刃边靶标本身并不包含频率成分,需求导来恢复,引入计算误差与噪声,降低了 MTF 检测精度^[12-14],通过获取光学遥感卫星成像系统线扩散函数的半最大值全宽确定地面像元分辨率时,易受大气影响而检测精度不高。针对光学遥感卫星像质评价方法的不足,提出基于阵列点源的在轨像质评价方法,以期提高光学遥感卫星图像质量评价精度。

阵列点源法像质评价是根据调制传递函数物理定义进行的直接检测方法,沿遥感器飞行方向与其探测器线阵方向分别布设非整数像素间隔的反射点源检测参照目标,构成循环矩阵以获取成像系统的二维点扩散函数(Point Spread Function, PSF)与 MTF,结合地面点源布设点位的高精度测量,可同时获取光学遥感卫星的地面像元分辨率。

基金项目:国家自然科学基金(No. 41601388)

第一作者:郑昱君, yujunzheng@mail.ustc.edu.cn

通讯作者:徐伟伟, weilxu@aiofm.ac.cn

收稿日期:2022-10-14;录用日期:2022-12-27

<http://www.photon.ac.cn>

1 基本原理

阵列点源目标可将近似平行入射的太阳光发散一定的角度,便于光学遥感卫星观测成像。经光学追迹与数值模拟,遥感器接收的反射光仅为点源目标的一小区域,尺度约为厘米或毫米量级,相对于米量级或亚米量级地面像元分辨率的光学遥感卫星来说,可作为点激冲光源对其进行像质评价。光学遥感卫星成像系统可作为线性位移不变系统,地物目标与输出图像之间的物像关系可以表示为

$$g(x, y) = f(x, y) * h(x, y) + b = h(x, y) + b \quad (1)$$

式中, (x, y) 为图像空间坐标, $g(x, y)$ 为输出图像, $f(x, y)$ 为地物目标, $*$ 为卷积符号, $h(x, y)$ 为系统点扩散函数, b 为背景值。

由式(1)可知,光学遥感卫星对地面反射点源目标观测成像输出结果表现为卫星成像系统自身的点扩散特性,即可根据调制传递函数的物理定义对其进行像质评价。

光学遥感卫星成像系统主要由光学子系统、探测器子系统、电子学子系统等组成,此外还受卫星平台运动影响,基于傅里叶光学及卷积定理,表征系统自身特性的点扩散函数是各组成部分点扩散函数的卷积^[15]。根据文献调研,结合光学遥感卫星的恒星观测及地面点源成像等试验^[16-19],可近似采用高斯模型来表征光学遥感卫星成像系统的点扩散特性,故遥感成像系统对地面点源目标成像后的输出图像可表示为

$$g(x, y) = k \exp \left[-\frac{(x-x_0)^2}{2\sigma^2} - \frac{(y-y_0)^2}{2\zeta^2} \right] + b \quad (2)$$

式中, k 为系数因子, (x_0, y_0) 为峰值坐标, (σ, ζ) 为横向与纵向的标准偏差。

根据光学遥感卫星成像系统的物像关系并结合点源遥感影像,通过最小二乘法进行二维高斯模型拟合可确定每个反射点源影像的峰值位置,即

$$\epsilon_{\min} = \sum_{i=1}^n \sum_{j=1}^m \left\{ g(x_i, y_j) - k \exp \left[-\frac{(x_i-x_0)^2}{2\sigma^2} - \frac{(y_j-y_0)^2}{2\zeta^2} \right] - b \right\}^2 \quad (3)$$

式中, $g(x_i, y_j)$ 为点源图像中空间坐标为 (x_i, y_j) 的像素点计数值。

根据几何关系可知,光学遥感卫星沿轨或垂轨方向的点源目标的地面间距与其相应的卫星影像中像点间距之比即为地面像元分辨率

$$D_{\text{gsd}} = \frac{\sqrt{(X_{k+1} - X_k)^2 + (Y_{l+1} - Y_l)^2 + (Z_{q+1} - Z_q)^2}}{\sqrt{(x_{k0+1} - x_{k0})^2 + (y_{l0+1} - y_{l0})^2}} \quad (4)$$

式中, (X_k, Y_l, Z_q) , $(X_{k+1}, Y_{l+1}, Z_{q+1})$ 为地面点源坐标,可采用实时动态全球定位系统(Real Time Kinematic-Global Positioning System, RTK-GPS)高精度测量, (x_{k0}, y_{l0}) , (x_{k0+1}, y_{l0+1}) 为对应地面点源的卫星影像的像点坐标。

光学遥感卫星在轨 MTF 检测时,通常采用非整数像素间隔的反射点源阵列构成循环矩阵,以联合光学卫星相机多个探测元对其进行扫描成像。以每个点源影像的峰值点坐标(或相对相位)为基准将所有点源影像数据进行位置配准,获取过采样的、亚像素插值的光学遥感卫星成像系统点扩散轮廓,克服目前广泛应用于遥感的光电成像系统采样效应的影响,以准确恢复出遥感成像系统的点扩散函数,进而获取系统调制传递函数,提高遥感卫星在轨像质评价精度^[20-21]。通过最小二乘法对重排后的图像数据进行二维高斯曲面拟合便可获取成像系统点扩散函数,由 MTF 的物理定义,系统点扩散函数经离散傅里叶变换得到系统 MTF,即

$$M_{\text{MTF}}(\nu, \xi) = \left| \text{DFT} \left[g(x, y) \right] \right| \quad (5)$$

式中, M_{MTF} 为系统 MTF, (ν, ξ) 分别为纵向与横向频率, $\text{DFT}(\bullet)$ 为离散傅里叶变换。

2 在轨检测试验

资源三号卫星基于反射点源的像质评价试验中,在定标试验场沿飞行方向与探测器线阵方向集中布设

4×4的非整像素间隔的反射点源阵列,相邻点源间距为10.25像素,相间点源间距为20.5像素,如图1所示。根据基本原理中所述,当沿遥感器飞行方向布设4×4阵列的非整数像素间隔的点源目标时,光学遥感成像系统点扩散函数可亚像素插值至0.25像素,能够有效克服成像系统采样效应与抑制随机噪声影响,准确地恢复出光学遥感卫星成像系统的点扩散函数,进而获取系统调制传递函数。在轨检测试验通常选择在大气干洁、晴朗无云的天气条件下进行,根据轨道预报,光学遥感卫星星下点观测成像,获取试验遥感影像,如图2所示。采用RTK-GPS对每个反射点源目标的中心位置进行高精度测量,以获取反射点源的地面坐标与实际间距,探测器线阵与卫星飞行方向相邻点源地面间距如表1所示。

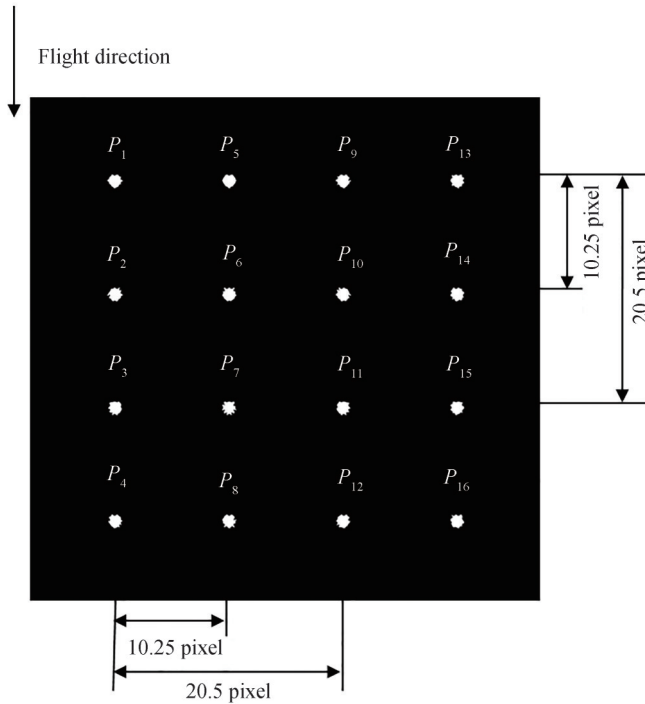


图1 阵列点源布设示意图
Fig. 1 Deployment of an array of point sources

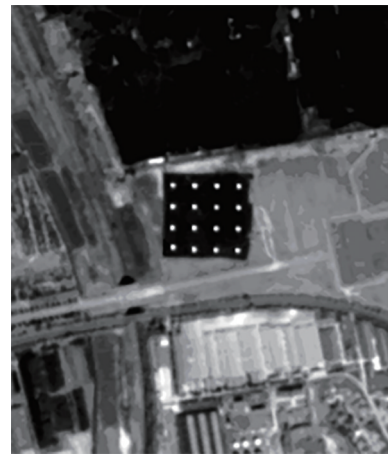


图2 遥感影像
Fig.2 Remote sensing image

表1 地面相邻反射点源间距

Table 1 Distances of ground adjacent reflected point source

Direction	Segment	Distance/m	Segment	Distance/m	Segment	Distance/m
Linear array	P_1-P_5	35.875 0	P_5-P_9	35.863 5	P_9-P_{13}	35.877 9
	P_2-P_6	35.871 0	P_6-P_{10}	35.867 6	$P_{10}-P_{14}$	35.870 2
	P_3-P_7	35.851 9	P_7-P_{11}	35.913 4	$P_{11}-P_{15}$	35.876 1
	P_4-P_8	35.861 0	P_8-P_{12}	35.874 9	$P_{12}-P_{16}$	35.869 7
Flight	P_1-P_2	35.878 2	P_2-P_3	35.874 5	P_3-P_4	36.262 9
	P_5-P_6	35.843 2	P_6-P_7	35.905 1	P_7-P_8	36.252 8
	P_9-P_{10}	35.854 9	$P_{10}-P_{11}$	35.896 3	$P_{11}-P_{12}$	36.237 6
	$P_{13}-P_{14}$	35.909 1	$P_{14}-P_{15}$	35.860 3	$P_{15}-P_{16}$	36.238 8

反射点源主要由反射镜组件、太阳敏感器、姿态调控组件与控制软件系统等组成,可将入射至点源反射镜的太阳光束反射至光学遥感卫星入瞳,形成点激冲辐射。根据遥感器动态范围,结合光学遥感卫星可接收能量要求,经点源目标反射至遥感器入瞳能量与经地表反射至遥感器入瞳能量相匹配,据此设计反射镜在太阳反射波段的镜面反射率优于90%,使得反射点源目标反射适量光通量在光学卫星相机响应高端且不饱和,并具有较好的信噪比;根据卫星轨道预报精度与反射点源指向精度等,并考虑一定角度冗余,保障过顶时刻遥感器能够接收到经点源反射的太阳光束的情况下,设计反射镜尺度小于遥感器地面像元分辨率的

10%,以实现轻量化、小型化的反射点源。通过太阳传感器对太阳运动轨迹的自动跟踪观测,实现精度优于 0.1° 的点源姿态调控误差校准与角度标校,可自动匹配太阳光-点源目标-光学遥感卫星间的光路^[22],准确获取地面反射点源的遥感影像。

根据反射点源遥感影像可知,如图3所示,每个点源影像响应值覆盖约 3×3 像素,选取每个反射点源遥感影像的 5×5 像素值则能够包含背景及点源目标的响应值。将25个像素值代入点扩散函数模型进行二维高斯曲面拟合,如图4所示,根据拟合结果获取点源图像的像点坐标,如表2所示,进而求得点源的像点间距。

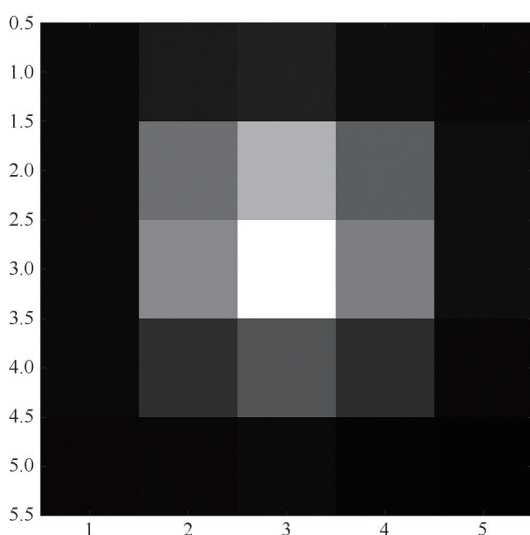


图3 反射点源影像
Fig. 3 Image of reflected point source

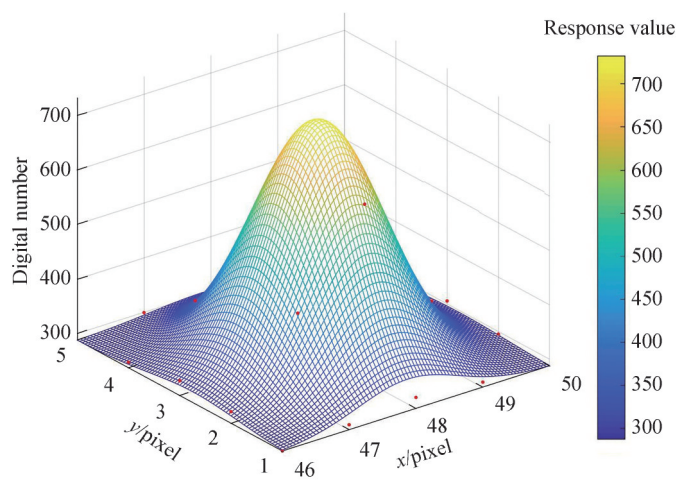


图4 曲面拟合
Fig. 4 Surface fitting

表2 反射点源像点坐标

Table 2 Pixel coordinates of reflected point source image

Parameter	P_1	P_2	P_3	P_4	P_5	P_6	P_7	P_8
X_0/Pixel	633.788	633.671	633.452	633.508	644.890	644.737	644.582	644.503
Y_0/Pixel	554.143	564.266	574.443	584.907	554.335	564.450	574.611	584.885
Parameter	P_9	P_{10}	P_{11}	P_{12}	P_{13}	P_{14}	P_{15}	P_{16}
X_0/Pixel	656.135	655.958	655.745	655.620	667.289	667.138	666.954	666.711
Y_0/Pixel	554.492	564.712	574.886	585.131	554.699	564.910	575.051	585.298

根据反射点源法地面像元分辨率检测原理,反射点源的地面间距与其遥感图像的像点间距相比即得遥感卫星的地面像元分辨率,如表3所示。光学遥感卫星的探测器线阵方向与飞行方向的地面像元分辨率分别为3.22 m和3.52 m,标准偏差分别为0.020 6和0.021 5,相对偏差分别为6.4‰和6.1‰,表明所测光学遥感卫星探元具有良好的稳定性与可靠性。

按照阵列点源像点坐标对 4×4 阵列点源影像数据进行位置配准,以获取亚像素插值的系统点扩散响应,即遥感器成像系统的点扩散轮廓,降低光电成像系统的采样效应与随机噪声对在轨MTF检测结果的影响,提高反射点源法像质评价精度。如图5所示,通过参数化高斯模型拟合即可获取系统点扩散函数,对其进行傅里叶变换取模并归一化即得光学遥感卫星系统MTF,如图6所示。采用阵列点源法对资源三号卫星进行在轨MTF检测的结果与采用双边缘线状地物法对资源三号卫星进行在轨MTF检测的结果^[23](飞行方向0.147 4,线阵方向0.143 4)在遥感器飞行方向与线阵方向的差异分别为0.000 2与0.012 6,具有较好的一致性。

表3 地面像元分辨率
Table 3 Ground pixel resolution

Direction	Segment	Ground pixel resolution/m	Segment	Ground pixel resolution/m	Segment	Ground pixel resolution/m
Linear array	P_1-P_5	3.230 9	P_5-P_9	3.189 0	P_9-P_{13}	3.216 0
	P_2-P_6	3.241 1	P_6-P_{10}	3.195 6	$P_{10}-P_{14}$	3.207 9
	P_3-P_7	3.220 8	P_7-P_{11}	3.216 2	$P_{11}-P_{15}$	3.200 3
	P_4-P_8	3.261 6	P_8-P_{12}	3.226 2	$P_{12}-P_{16}$	3.233 8
		Average 3.22	Standard deviation 0.020 6		Relative standard deviation 6.4‰	
Flight	P_1-P_2	3.544 0	P_2-P_3	3.524 2	P_3-P_4	3.465 4
	P_5-P_6	3.543 2	P_6-P_7	3.533 2	P_7-P_8	3.528 5
	P_9-P_{10}	3.507 8	$P_{10}-P_{11}$	3.527 5	$P_{11}-P_{12}$	3.536 8
	$P_{13}-P_{14}$	3.516 3	$P_{14}-P_{15}$	3.535 6	$P_{15}-P_{16}$	3.535 5
		Average 3.52	Standard deviation 0.021 5		Relative standard deviation 6.1‰	

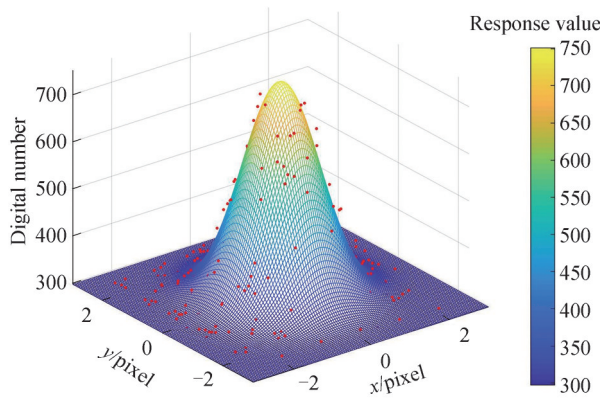


图5 点扩散函数
Fig. 5 Point spread function

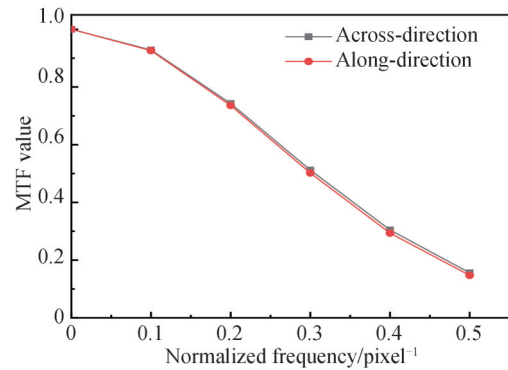


图6 系统MTF
Fig. 6 System MTF

3 分析与讨论

光学遥感卫星阵列点源法像质评价是以“小”而“亮”的自动化反射点源作为检测参照,沿传感器飞行方向与探测器线阵方向按照非整像素间隔阵列化布设并测量地面点源坐标,结合点源遥感影像对光学卫星图像质量评价参数进行在轨检测。像质评价精度与点源结构形式、像点检测精度等因素有关,分析讨论这些影响的同时,结合地面同步(准同步)观测的大气参数等,可实现遥感器的在轨辐射定标。

反射点源既有相对传感器分辨率小得多的尺度,又有相对地面目标背景高得多的辐射,可自动实现太阳光-阵列点源-光学遥感卫星间的光路对准,便于成像且信噪比高。用于LANDSAT TM相机的漫射点源(高反射率背景中的低反射率点源目标),尺寸为传感器地面像元分辨率的一半,按照非整像素间隔布设为 4×4 阵列,易受背景及噪声影像且信噪比较差^[24-25],相较之下,反射点源具有较高的辐射亮度且信噪比高;用于SPOT卫星的主动点源(姿态可调的高能量的聚光灯),需要多次观测成像来克服光学遥感卫星采样效应影响,易受大气状况与光谱非一致性影响^[9,26],相较之下,反射点源无需对辐射能量进行定标,不存在与太阳反射波段光谱的非一致性,且无需大功率电源供电;用于IKONO卫星的深空恒星,对卫星姿态控制技术与轨道调整技术要求较高,相较之下,使用反射点源时无需进行卫星平台翻转或姿态调整^[27]。

在阵列点源法像质评价试验中,点源目标中心的横向或纵向连线应在一条直线上,据此根据共线检验原则,相邻反射点源中心的距离和应与相间反射点源中心的距离相等。如表4所示,光学遥感卫星探测器线阵与飞行方向共线检验结果误差均小于0.002像素,表明阵列点源像点提取与地面像元分辨率检测结果均具有较高的精度与准确性。地面像元分辨率是反射点源地面间距与其影像像点间距之比,该比例系数也可

作为点源影像像点检测精度的验证参数,如表3所示,具有较好的一致性,在光学遥感卫星探测器线阵方向与飞行方向的标准偏差分别为0.020 6和0.021 5,相对偏差分别为6.4%和6.1%,表明点源影像像点提取精度高,遥感器线阵探测元在局部范围内具有较好的刚性与稳定性。

表4 共线检测
Table 4 Co-linear detection

Direction	Co-linear relationship	Result	Co-linear relationship	Result
Linear array	$P_1P_5 + P_5P_9 - P_1P_9$	3.10×10^{-5}	$P_5P_9 + P_9P_{13} - P_5P_{13}$	5.91×10^{-5}
	$P_1P_9 + P_9P_{13} - P_1P_{13}$	3.22×10^{-5}	$P_1P_5 + P_5P_{13} - P_1P_{13}$	4.04×10^{-5}
	$P_2P_6 + P_6P_{10} - P_2P_{10}$	1.26×10^{-4}	$P_6P_{10} + P_{10}P_{14} - P_6P_{14}$	8.90×10^{-5}
	$P_2P_{10} + P_{10}P_{14} - P_2P_{14}$	1.97×10^{-5}	$P_2P_6 + P_6P_{14} - P_2P_{14}$	5.65×10^{-5}
	$P_3P_7 + P_7P_{11} - P_3P_{11}$	2.53×10^{-4}	$P_7P_{11} + P_{11}P_{15} - P_7P_{15}$	2.75×10^{-4}
	$P_3P_{11} + P_{11}P_{15} - P_3P_{15}$	9.89×10^{-5}	$P_3P_7 + P_7P_{15} - P_3P_{15}$	7.77×10^{-5}
	$P_4P_8 + P_8P_{12} - P_4P_{12}$	1.61×10^{-3}	$P_8P_{12} + P_{12}P_{16} - P_8P_{16}$	1.39×10^{-4}
	$P_4P_{12} + P_{12}P_{16} - P_4P_{16}$	8.96×10^{-5}	$P_4P_8 + P_8P_{16} - P_4P_{16}$	1.51×10^{-3}
Flight	$P_1P_2 + P_2P_3 - P_1P_3$	2.52×10^{-4}	$P_2P_3 + P_3P_4 - P_2P_4$	1.86×10^{-3}
	$P_1P_3 + P_3P_4 - P_1P_4$	1.66×10^{-3}	$P_1P_2 + P_2P_4 - P_1P_4$	4.02×10^{-5}
	$P_5P_6 + P_6P_7 - P_5P_7$	4.17×10^{-8}	$P_6P_7 + P_7P_8 - P_6P_8$	1.46×10^{-4}
	$P_5P_7 + P_7P_8 - P_5P_8$	1.92×10^{-4}	$P_5P_6 + P_6P_8 - P_5P_8$	4.57×10^{-5}
	$P_9P_{10} + P_{10}P_{11} - P_9P_{11}$	3.33×10^{-5}	$P_{10}P_{11} + P_{11}P_{12} - P_{10}P_{12}$	1.94×10^{-4}
	$P_9P_{11} + P_{11}P_{12} - P_9P_{12}$	1.63×10^{-4}	$P_9P_{10} + P_{10}P_{12} - P_9P_{12}$	2.0×10^{-6}
	$P_{13}P_{14} + P_{14}P_{15} - P_{13}P_{16}$	2.86×10^{-5}	$P_{14}P_{15} + P_{15}P_{16} - P_{14}P_{16}$	7.9×10^{-5}
	$P_{13}P_{15} + P_{15}P_{16} - P_{13}P_{16}$	1.79×10^{-4}	$P_{13}P_{14} + P_{14}P_{16} - P_{13}P_{16}$	1.29×10^{-4}

基于阵列点源的光学遥感卫星像质评价方法是根据调制传递函数的物理定义进行的直接检测方法,可以直观表征遥感器点扩散特性或模糊特性,获取成像系统调制传递函数的同时,结合地面测量得到的阵列点源位置坐标还可得地面像元分辨率。相较基于三线靶标或辐射状靶标的光学遥感卫星像质评价方法,可避免主观判断可分辨-不可分辨点的影响,且可获得遥感器成像系统的全频率MTF值;相较常用的基于倾斜刃边的光学遥感卫星像质评价方法无需求导恢复各频率,避免多步骤数据处理引入额外误差,抑制大气与噪声对检测结果的影响,具有较高的像质评价精度。

光学遥感卫星基于阵列点源的在轨像质评价,结合大气光学特性参数地面同步或准同步自动化观测,通过简化辐射传输计算建立点源目标反射至遥感器的入瞳辐亮度与点源影像响应值间的定量关系,进而实现基于反射点源的辐射定标。根据地面同步或准同步观测的大气光学特性参数,结合气象信息与点源目标反射率等参数,经辐射传输计算获取经点源反射至遥感器入瞳的辐亮度,再结合光学遥感卫星相机的光谱响应函数获得等效辐亮度;阵列点源遥感影像经点扩散函数拟合与统计分析获取点源影像计数统计值,结合多级点源目标的线性回归可有效分离出点源目标响应值与背景辐射响应值;进而由遥感器入瞳等效辐亮度与点源目标响应值结合辐射定标方程获取光学遥感卫星的定标系数,实现光学遥感卫星基于阵列点源的自动化辐射定标^[28]。

4 结论

光学遥感卫星阵列点源法像质评价是以轻小型、自动化的反射点源阵列作为检测参照,同时获取遥感器地面像元分辨率与MTF等像质评价参数的在轨检测方法。试验结果表明,采用二维高斯曲面拟合方法进行点源像点坐标提取的精度较高,光学遥感器探测器线阵与飞行方向的共线检测误差小于0.002像素,地面像元分辨率的检测结果小于6.5%。阵列点源法是根据MTF物理定义进行的在轨MTF检测方法,通过像点提取、数据配准、二维高斯曲面拟合、傅里叶变换等步骤直接获取表征遥感器成像系统点扩散特性的二维PSF以及全频率的二维MTF,能够全面反应成像系统的成像能力,克服了利用三线靶标法或辐射状靶标法仅能获取单点MTF值以及利用倾斜刃边法在求导过程中引入计算误差与噪声的缺点。同时,结合地面

点源坐标的高精度测量,阵列点源法可以定量检测光学遥感卫星的地面像元分辨率,避免了利用三线靶标法或辐射状靶标法人工判定可分辨-不可分辨点以及利用倾斜刃边法时大气对检测结果的影响,提高了地面像元分辨率检测精度。此外,阵列点源还可以作为光学遥感卫星辐射定标的参考目标,通过地面设置多能级点源阵列,结合大气光学特性参数测量,实现遥感器在轨辐射定标。因此,阵列点源有望综合实现光学遥感卫星的辐射定标与像质评价。

参考文献

- [1] XU Weiwei, ZHANG Liming, LI Xin, et al. On-orbit absolute radiometric calibration of high resolution satellite optical sensor based on gray-scale targets[J]. *Infrared and Laser Engineering*, 2018, 47(4): 0417005.
徐伟伟, 张黎明, 李鑫, 等. 基于灰阶靶标的高分辨光学卫星传感器在轨绝对辐射定标[J]. *红外与激光工程*, 2018, 47(4): 0417005.
- [2] LEGER D, VIALLEFONT F, DELIOT P, et al. On-orbit MTF assessment of satellite cameras[M]. London: Taylor & Francis Group, 2004: 67-76.
- [3] PENG Yu, HUANG Haile, ZHU Leiming. The in-orbit resolution detection of TH-01 CCD cameras based on the radial target[J]. *Geomatics & Spatial Information Technology*, 2013, 36(7): 149-151.
彭宇, 黄海乐, 朱雷鸣. 基于辐射状靶标的天绘一号卫星 CCD 相机分辨率在轨检测[J]. *测绘与空间地理信息*, 2013, 36(7): 149-151.
- [4] XU Weiwei, ZHANG Liming, SHEN Zhengguo, et al. On-orbit MTF estimation of high resolution satellite optical sensor[J]. *Journal of Atmospheric and Environmental Optics*, 2014, 9(2): 97-111.
徐伟伟, 张黎明, 沈政国, 等. 高分辨光学卫星传感器在轨 MTF 检测[J]. *大气与环境光学学报*, 2014(2): 97-111.
- [5] XU Weiwei, ZHANG Liming, SI Xiaolong, et al. Image-quality evaluation of high-spatial-resolution satellite optical sensor based on radial target[J]. *Acta Optica Sinica*, 2019, 39(9): 0928003.
徐伟伟, 张黎明, 司孝龙, 等. 基于辐射状靶标的高分辨率光学卫星传感器像质评价方法研究[J]. *光学学报*, 2019, 39(9): 0928003.
- [6] CHOI T. IKONOS satellite on orbit modulation transfer function (MTF) measurement using edge and pulse method[D]. South Dakota: South Dakota State University, 2002.
- [7] KOHM K. Modulation transfer function measurement method and results for the Orbview-3 high resolution imaging satellite[C]. *ISPRS*, 2004, 35: 12-23.
- [8] XU Weiwei, ZHANG Liming, SI Xiaolong, et al. On-orbit modulation transfer function detection of high resolution optical satellite sensor based on reflected point sources[J]. *Acta Optica Sinica*, 2017, 37(7): 0728001.
徐伟伟, 张黎明, 司孝龙, 等. 基于反射点源的高分辨率光学卫星传感器在轨调制传递函数检测[J]. *光学学报*, 2017, 37(7): 0728001.
- [9] LEGER D, DUFFAUT J, ROBINET F. MTF measurement using spotlight[C]. *IEEE International Geoscience and Remote Sensing Symposium*, 1994, 4: 2010-2012.
- [10] LI X B, JIANG X G, TANG L L. On-orbit MTF estimation methods for satellite sensors[C]. *Asia-Pacific Space Outlook*, 2007, 2: 38-43.
- [11] XU Weiwei, ZHANG Liming, YANG Benyong, et al. On-orbit MTF measurement of high resolution satellite optical camera using periodic targets[J]. *Acta Optica Sinica*, 2011, 31(7): 0711001.
徐伟伟, 张黎明, 杨本永, 等. 基于周期靶标的高分辨光学卫星相机在轨 MTF 检测方法[J]. *光学学报*, 2011, 31(7): 0711001.
- [12] CHOI T, HELDER D. Generic sensor modeling for modulation transfer function (MTF) estimation[J]. *Pecora 16 Global Priorities in Land Remote Sensing*, 2005: 1-12.
- [13] NELSON N R, BARRY P S. Measurement of hyperion MTF from on-orbit scenes[C]. *IEEE International Geoscience and Remote Sensing Symposium*, 2001, 7: 2967-2969.
- [14] LELOGLU U M, TUNALI E. On-orbit modulation transfer function estimation for BILSAT imagers [C]. *ISPRS*, 2006: 45-51.
- [15] XU Weiwei. On-orbit MTF estimation of high resolution satellite optical sensor [D]. Beijing: University of Chinese Academy of Sciences, 2011.
徐伟伟. 高分辨光学卫星传感器在轨 MTF 检测方法研究[D]. 北京: 中国科学院大学, 2011.
- [16] SCHOWENGERDT R A. *Remote sensing: models and methods for image processing*[M]. San Diego: Academic Press, 2007.
- [17] MIGHELL K J. The MATPHOT algorithm for digital point spread function CCD stellar photometry[C]. *International Society for Optics and Photonics*, 2002, 4847: 207-216.
- [18] SCHOWENGERDT R A. Spatial response of the EO-1 advanced land imager (ALI)[C]. *IEEE International Geoscience and Remote Sensing Symposium*, 2002, 6: 3121-3123.

- [19] XU Q, SCHOWENGERDT R A. Urban targets for image quality analysis of high-resolution satellite imaging systems[C]. SPIE, 2003, 5108: 31-38.
- [20] WANG Xianhua, QIAO Yanli, WANG Leyi, et al. In-flight MTF measurement of satellite-board CCD camera [J]. Chinese Journal of Quantum Electronics, 2005, 22(1): 106-110.
王先华, 乔延利, 王乐意, 等. 基于小靶标法的星载 CCD 相机 MTF 在轨检测研究[J]. 量子电子学报, 2005, 22(1): 106-110.
- [21] ROBINET F, LEGER D, CERBELAUD H, et al. Obtaining the MTF of a CCD imaging system using an array of point sources: evaluation of performances[C]. IEEE IGARSS'91 Remote Sensing: Global Monitoring for Earth Management, 1991, 3: 1357-1361.
- [22] LI Ruijin. Research on radiation calibration method and system of satellite remote sensing point light source[D]. Hefei: University of Science and Technology of China, 2021.
李瑞金. 卫星遥感点光源辐射标校方法与系统研究[D]. 合肥: 中国科学技术大学, 2021.
- [23] WANG Chang, GU Xingfa, YU Tao, et al. On-orbit MTF measurement and image restoration for ZY-3 satellite [J]. Computer Engineering, 2014, 40(4): 237-241.
汪畅, 顾行发, 余涛, 等. 资源三号卫星在轨 MTF 测量与图像复原[J]. 计算机工程, 2014, 40(4): 237-241.
- [24] RAUCHMILLER JR R F, SCHOWENGERDT R A. Measurement of the landsat thematic mapper MTF using a 2-dimensional target array[C]. SPIE, 1986, 697: 105-114.
- [25] RAUCHMILLER JR R F, SCHOWENGERDT R A. Measurement of the Landsat Thematic Mapper modulation transfer function using an array of point sources[J]. Optical Engineering, 1988, 27(4): 334-343.
- [26] LEGER D, VIALLEFONT F, HILLAIRET E, et al. In-flight refocusing and MTF assessment of SPOT5 HRG and HRS cameras[C]. SPIE, 2003, 4881: 224-231.
- [27] BOWEN H S, DIAL G. IKONOS calculation of MTF using stellar images [J]. Proceedings of the 2002 High Spatial Resolution Commercial Imagery Evaluation Team, 2002.
- [28] XU Weiwei, ZHANG Liming, CHEN Hongyao, et al. In-flight radiometric calibration of high resolution optical satellite sensor using reflected point sources[J]. Acta Optica Sinica, 2017, 37(3): 0328001.
徐伟伟, 张黎明, 陈洪耀, 等. 基于反射点源的高分辨率光学卫星传感器在轨辐射定标方法[J]. 光学学报, 2017, 37(3): 0328001.

Image Quality Evaluation Method for Optical Remote Sensing Satellite Based on an Array of Point Sources

ZHENG Yujun^{1,2}, XU Weiwei¹, LI Xin¹, SI Xiaolong¹, YANG Baoyun¹, ZHANG Liming¹
(1 Key Laboratory of Optical Calibration and Characterization, Hefei Institutes of Physical Science, Chinese Academy of Science, Hefei 230031, China)
(2 University of Science and Technology of China, Hefei 230026, China)

Abstract: Ground pixel resolution and modulation transfer function are two important parameters for image quality evaluation of high spatial resolution optical remote sensing satellites, which are of great significance in target recognition, image interpretation, and information extraction. We present an image quality evaluation method for remote sensor using an array of point sources, which takes the light, small, and automated reflected point source array as reference. Two image quality evaluation parameters of remote sensor ground pixel resolution and modulation transfer function can be obtained at the same time. The two-dimensional Gaussian model is used to describe the point spread characteristic of the optical remote sensing satellite imaging system. Selecting the 5×5 pixel values of each reflective point source remote sensing image into the point spread function model and use the least squares method to fit the two-dimensional Gaussian surface to obtain the image point coordinates. According to the ground pixel resolution detection principle and combined with the ground point source position measurement, the ground pixel resolution of the remote sensor is obtained. Based on the image point coordinates, all point source image data are positionally registered, and the image data after data rearrangement is fitted again with the two-dimensional Gaussian surface to obtain oversampled, sub-pixel interpolated optical remote sensing satellite imaging system point spread function, and then obtain the system modulation transfer function. In the

image quality evaluation test of ZY-3 satellite based on reflective point sources, a 4×4 reflective point source array with non-integer pixel intervals was concentrated on the calibration test site along the flight direction and the linear array direction. The distance between adjacent point sources is 10.25 pixels, and the distance between two point sources is 20.5 pixels. The point spread function of the optical remote sensing imaging system can be sub-pixel interpolated to 0.25 pixels, which can effectively overcome the sampling effect of the imaging system and suppress the influence of random noise. According to the principle of collinearity test, the sum of the centers of adjacent reflection point sources should be equal to the distance between the centers of phase reflection point sources. The test results show that the error of the collinearity test results between the optical remote sensing satellite detector linear array and the flight direction is less than 0.002 pixels. It shows that the extraction result of array point source image point has high precision and accuracy. The standard deviations of the ground pixel resolution detection results in the linear array direction and flight direction of optical remote sensing satellite detectors are 0.020 6 and 0.021 5, relative deviations are 6.4‰ and 6.1‰, which shows that the point source image pixel extraction accuracy is high and the linear array detection element of the remote sensor has good rigidity and stability in a local area. Comparing the results of the on-orbit modulation transfer function detection of the ZY-3 satellite by the array point sources method and the double-edge method, the difference between the two methods in the flight direction and the linear array direction is 0.000 2 and 0.012 6. Compared with periodic targets, array point sources have the characteristics of light weight, miniaturization, and automation. In the process of quantitative detection of the ground pixel resolution of optical remote sensing satellites, the array point source method is not affected by the subjective factors of image interpreters and can suppress the influence of atmospheric and random noise. The array point source method is a two-dimensional modulation transfer function direct detection method according to the physical definition of modulation transfer function, which can intuitively describe the point spread characteristic of the photoelectric remote sensing imaging system. The array point sources can also be used as a reference target for the radiometric calibration of optical remote sensing satellites. The on-orbit radiometric calibration of remote sensors can be realized by setting up a multi-level point source array on the ground, combined with the measurement of atmospheric optical characteristic parameters. Therefore, the array point sources can comprehensively realize the image quality evaluation and radiometric calibration of optical remote sensing satellites.

Key words: Remote sensing; Image quality evaluation; Modulation transfer function; Ground pixel resolution; Array of point sources

OCIS Codes: 280.4788; 110.3000; 110.4850; 350.5730